

Treatment of Dye Laden Wastewater through Electrocoagulation: Effect of Control Factors and Process Optimization



Submitted by:

**Adnan Akhtar
2017-MS-CH-05**

Supervisor:

Dr. Hafiz Muhammad Zaheer Aslam

**Department of Chemical Engineering
University of Engineering and Technology, Lahore**

This Page is left blank intentionally

Table of Contents

List of Figures.....	V
List of Table.....	VI
ACKNOWLEDGEMENT.....	VII
Abstract.....	VIII
1. Introduction and Literature Review:	2
2. Material and Methods	6
2.1 Chemicals	6
2.2 Pre-treatment of Electrodes	6
2.3 Experimental Set-up and Experimentation.....	6
2.4 Analytical Procedure	7
2.5 Experimental Design and Response Surface Methodology	8
3. Results and Discussion	11
3.1 Model Development and Statistical Analysis.....	11
3.2 Pareto Analysis.....	15
3.3 Perturbation Plots	16
3.4 Effect of Operating Parameters	18
3.4.1 Effect of initial pH	19
3.4.2 Effect of Inter-electrode spacing	21
3.5 Optimization including desirability and kinetic analysis	25
3.6 Concentration of residual iron post EC Process.....	29
3.7 FTIR Analysis of Standard dye and Residual Sludge.....	31
4. Conclusion	33
5. References	33

List of Figures

Fig. 1 Schematic Diagram of EC cell: (1) DC supply, (2) Magnetic Bar, (3) Dye polluted wastewater sample, (4) Magnetic stirrer.....	7
Fig. 2 Actual vs predicted values plot for testing Adequacy of developed regression models describing (a) COD reduction (b) Color Removal Efficiency of EC Process	14
Fig. 3 Graphical Pareto Plot of independent variables on selected responses	16
Fig. 4 Perturbation Plots at center point of design space for (a) COD reduction efficiency (b) Color removal efficiency. *Where A, B and C represents Initial concentration of dye (mg/L), Inter-electrode spacing (cm) and pH.....	18
Fig. 5 Three-dimensional response surface plots of %COD reduction between (a) electrode spacing and initial concentration of dye (b) electrode spacing and pH (c) pH and initial concentration of dye.....	23
Fig. 6 Three-dimensional response surface plots of %Decolorization between (a) electrode spacing and initial concentration of dye (b) electrode spacing and pH (c) pH and initial concentration of dye.....	24
Fig. 7 EC Performance with respect to electrolysis time (pH=3; I.E Spacing= 3cm; Initial concentration of dye=1000 mg/L)	26
Fig. 8 Graphical Plots of a) Zero-order b) First-order and c) Second-order Kinetic Models for COD reduction under optimum parameters (Initial Concentration of dye=1000mg/L ; Initial pH=3 ; Inter-electrode distance=2.8 cm)	29
Fig. 9. Concentration of Residual with respect to different sequence of experiments	31
Fig. 10.FTIR Spectra of Standard Congo Red dye (a) and Residual Sludge (b) obtained after EC process (pH=3; Inter-electrode spacing= 3cm ; Initial concentration of dye= 1000 mg/L)	32

List of Table

Table 1: Ranges and Levels of Independent Variables.....	9
Table 2 Factors and Responses from RSM.....	12
Table 3 Regression estimate of selected model for COD reduction and Color removal.....	13
Table 4. ANOVA analysis for %COD and %Decolorization for EC process.....	15
Table 5. Effect of operating parameters on %COD and %Decolorization.....	18
Table. 6 Values of numerical optimization.....	27
Table.7. Concentration of iron residual against varied operating parameters.....	31

ACKNOWLEDGEMENT

First of all, I would like to thank Almighty Allah for providing me strength and blessing of creativity in order to pursue and accomplish my research work. After Allah's guidance, all respects are for our Holy Prophet Muhammad (PBUH) whose way of life and teachings are true source of knowledge and learning for whole mankind including myself. I would like to thank Dr. Hafiz Muhammad Zaheer Aslam whose supervision played a massive key role throughout my research work. His profound research knowledge and vast experience in academia helped me a lot during my graduate research. His suggestions and instructions were very insightful and I have tried to take maximum advantage of our collaboration.

Today I am not only a better Chemical Engineer but a better human being due to his influences. I couldn't be prouder of my decision of selecting him as my major supervisor. Besides Dr. Hafiz Muhammad Zaheer Aslam, I would like to pay an homage to Dr. Anam Asghar who played a key role in giving me a creative direction regarding my research project. Her forte of knowledge regarding wastewater treatment truly helped me in pursuing my research work and her suggestions as co-supervisor massively improved my acquittance in particular research area. Both of my supervisors spotted and groomed my creativity and enhance my appetite for increasing innovative skills. I am very thankful to Mr. Zubair Malik of Environmental Engineering Laboratory who provided friendly environment in Laboratory and helped me in acquiring basic chemicals which were required in my research work. Department of Chemical Engineering and Honorable Chairman deserve massive compliments and my respect for providing me research facility in order to pursue my research project.

And Lastly, I would like to thank my parents whose prayers and encouragement in pursuing my preferred field truly made me a man that I am today. They told me to never give up and love the work that I do. Their hard work has been prevailed and I couldn't be happier of the fact that they are proud of what I have accomplished.

Abstract

Wastewater discharge from textile sector has raised certain concerns, resulting in an unavoidable trade-off between industrial growth and environmental degradation. According to statistics, textile sector generates 200-350 m³ of wastewater per ton of finished product which results in higher COD ranging from 300-10,000 mg/L. Advanced Oxidation Processes (AOPs) are effective treatment methods for degradation of the recalcitrant wastewater. These processes involve the formation of hydroxyl radical which is highly oxidative and non-selective for most of the organic pollutants. However, high chemical consumption simultaneous with high energy requirements limits their industrial applications. Thus, in order to trade-off chemical consumption and energy equipment, electrocoagulation is identified a viable approach. In electrocoagulation, difference in electric potentials is utilized to generate coagulants which can remove color and other recalcitrant organic contaminants. It not only renders the consumption of chemicals but also reduces the sludge formation and thus reduces the operating cost of the process. Therefore, keeping these aspects in view, this study aims at treating dye laden wastewater through electrocoagulation using Iron (Fe) as electrode material. Congo red, an azo dye, was used as probe pollutant and central composite design was used to design and optimize the process conditions. The key parameters include initial dye concentration, pH and electrode distance were used to study their effects on decolorization and COD removal. According to experimental results, pH and electrode spacing were most significant factors with maximum COD and degradation efficiency of 90% and 97% respectively. Furthermore, the results showed that acidic conditions and inter electrode spacing have significant contribution towards overall performance of electrocoagulation and further process optimization may enhance the viability of this process due to the possibility of zero water discharge and reusability of dye in the textile sector.

CHAPTER 1: INTRODUCTION AND LITERATURE REVIEW

1. Introduction and Literature Review:

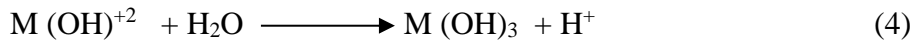
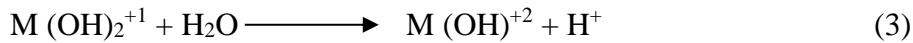
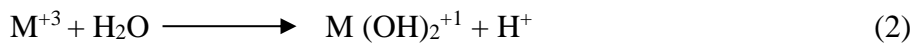
Wastewater discharged from textile industries has been one of the major problem for environmental contamination in many regions of the world. The chemical effluents generated within textile production sector are disposed as wastewater containing suspended solids and possess strong color due to the presence of residual dyes, high temperature, pH, turbidity and highly toxic chemicals. After getting discharged from the textile industry, wastewater gets mixed with fresh water reservoirs such as lakes and rivers. Therefore, pollutants in wastewater imparts daunting effects on aquatic environment due to reduction of oxygen supply within water[1]. Hence, there is a growing need for the removal of dye effluents from wastewater in order to ensure a healthy aquatic environment.

Various treatment techniques such as chemical coagulation/flocculation, advanced oxidation processes (AOPs), adsorption and biological treatment have been utilized for the removal of dye pollutant from wastewater. These processes have advantages as well as some limitations are observed simultaneously. Advanced Oxidation Processes such as electro-fenton oxidation, photo-catalysis, UV, ozonation, and sonolysis are the areas of great interest for wastewater treatment but these processes are complicated and high energy consumption possess major disadvantages[2]. Adsorption is another useful technique for wastewater treatment but it has complex regeneration process and high sludge disposal cost[3]. As textile effluents have low biodegradability at high concentration, it is necessary to perform pretreatment on wastewater before employing biological treatment[4]. Chemical coagulation is an economical method for treatment of dye wastewater through the use of okra mucilage as coagulant. However issues like adverse effects of chemicals, production of secondary pollutants within the process and high chemical utilization are major drawbacks faced in this process [5]. So, there is a growing need to develop more efficient and economical treatment methods that should consume less chemicals and installation space.

One of the most efficient treatment methods is electrocoagulation due to its numerous advantages. In electrocoagulation, difference in electric potentials is applied to generate coagulants which eliminate color and other recalcitrant organic contaminants. Electrocoagulation not only consumes less chemicals but also reduce sludge formation and operating cost of the process[6]. Moreover, electrocoagulation provides efficient rate of pollutant removal it is a simple process with less addition of chemicals. In recent years, electrocoagulation has been adopted for treatment of landfill leachate wastewater[7], paint manufacturing wastewater[8], tannery wastewater[9], paper mill wastewater[10] and removal

of various components such as arsenic[11], chromium[12] and phosphate[13],[14] from wastewater.

The basic mechanism of electrocoagulation includes the formation of coagulants in order to remove suspended solids, metals and dissolved solids from wastewater. If metal electrode is being utilized then metallic ions are generated at anode while hydrogen gas is released from the cathode side. Different types of ionic species such as $M(OH)^{+2}$, $M_2(OH)_2^{+4}$ and $M(OH)_4^{-1}$ are formed when these metallic ions remain in contact with water. These intermediate species are finally converted into $M(OH)_3$ known as coagulants after reacting with water. The overall procedure of coagulant formation can be described as follows:



Here M in these equations is type of metallic electrode used in electrochemical processes. Usually $Fe(OH)_3$ and $Al(OH)_3$ are coagulants which possess large surface area and high density for azo dyes. Settling time for the sludge is normally 24h in comparison with reaction time of 1 hour. So, as an alternative of the settling process, filtration technique has been used in order to separate sludge and suspended solids from treated wastewater.

Various research has been done using coagulation process for the removal of dye pollutant from textile wastewater. Verma et al. used Fe-Al composite electrode for textile wastewater containing dye solution comprising of reactive black 5 and disperse blue 3 along with various chemical additives. Through composite electrode, 90% of %COD was achieved[15]. Can et al. studied the use of poly aluminum chloride (PAC) and alum as chemical coagulant in Combined Electrocoagulation process (CEC). He concluded that 80% of %COD was achieved in CEC as compared to 23% in direct EC[16]. Similarly, GilPavas et al. used sequential chemical coagulation-electro-oxidation (CC-EO) method for the removal of dye pollutant from industrial textile wastewater and investigated the effects of different operating parameters such as pH, conductivity and current density. At optimum conditions in sequential CC-EO process, 93% and 100% of %COD and %Decolorization was achieved respectively[17]. Moreover, Alinsafi et al. proved that biodegradability of reactive dye like Drimarene K2LR CDG Blue can be increased by employing electrocoagulation by using Aluminum electrodes. Around

38.2% and 90.7% of %COD and %Decolorization was achieved by performing EC process[18]. From the extensive literature survey, it can be assessed that few studies have been focused on treatment performance of dye wastewater, with less emphasis have been employed on control factors involving initial concentration of dye, for COD removal and decolorization. As electrocoagulation can be applied on laboratory scale, effects of operating parameters and process optimization are essential for process development.

In the present research, treatment of azo dye pollutant Congo Red (CR) in wastewater has been performed through electrocoagulation. For electrocoagulation, Iron sheets were used as cathode and anode in the process. For experimental design, Response Surface Methodology (RSM) is a statistical experimental design method which is used in order to identify control variables for process optimization. Under RSM, Central Composite Design (CCD) technique is employed in order to design the process conditions and investigating the effects of independent variables such as pH, initial concentration of dye and inter-Electrode distance on selected responses including decolorization and Chemical Oxygen Demand (COD).

CHAPTER 2: MATERIALS AND METHODS

2. Material and Methods

2.1 Chemicals

Congo Red (Dye content $\geq 35\%$), with a molecular weight of 697 g/mol and λ_{\max} of 497 nm, was obtained from Sigma Aldrich, USA. In various experiments, NaOH (Pellets, 99% purity) and H₂SO₄ (98% purity, AR Grade), acquired from Merck KGaA, Darmstadt, Germany and Sigma Aldrich were used to control the initial pH of the reaction media. Anhydrous Sodium sulphate (Na₂SO₄, 99% purity) was also purchased from Sigma Aldrich. Acetone (99% purity, AR Grade, Merck KGaA Pvt. Ltd, Darmstadt, Germany) and HCl (37% purity, AR Grade, Sigma Aldrich, USA) were utilized for electrode cleaning. All the chemicals were of analytical grade and used as received.

2.2 Pre-treatment of Electrodes

Iron Sheets with dimension of 7cm×6cm and effective surface area of 42cm² were selected as electrode materials. Electrodes were initially cleaned with sand paper to remove corrosion from the surface. Later, Iron electrodes were submerged in Acetone for 20 minutes and then soaked in 3.0M HCl solution for 20 minutes for removal of grease and other impure particles from iron electrodes. Afterwards, electrodes were washed, rinsed with distilled water and dried for electrocoagulation experiments.

2.3 Experimental Set-up and Experimentation

Fig.1 shows the schematic diagram of batch electrocoagulation (EC) system. Experiments were conducted in a 500mL Pyrex glass beaker with two iron rods used as electrode materials. Electrodes were connected in parallel to a DC Power Supply (Dazheng, PS-605D, China), with current and voltage range of 0-2A and 0-80V respectively, in order to provide electric potential. For each experiment, 0.5 L of CR solution was taken and initial pH of the reaction media was set at desired values with H₂SO₄ (1 M) or NaOH (0.5 M) solution. The distance between electrodes was varied between 2 to 4 cm and constant mixing was done by using magnetic stirrer at 170 rpm. After 1 h, the power supply was turned off and solution was given sufficient time of 0.5 h for sludge settlement. Later, the supernatant was filtered and analyzed for decolorization, COD removal and iron content while sludge was analyzed for functional group analysis. All experiments were conducted at room temperature.

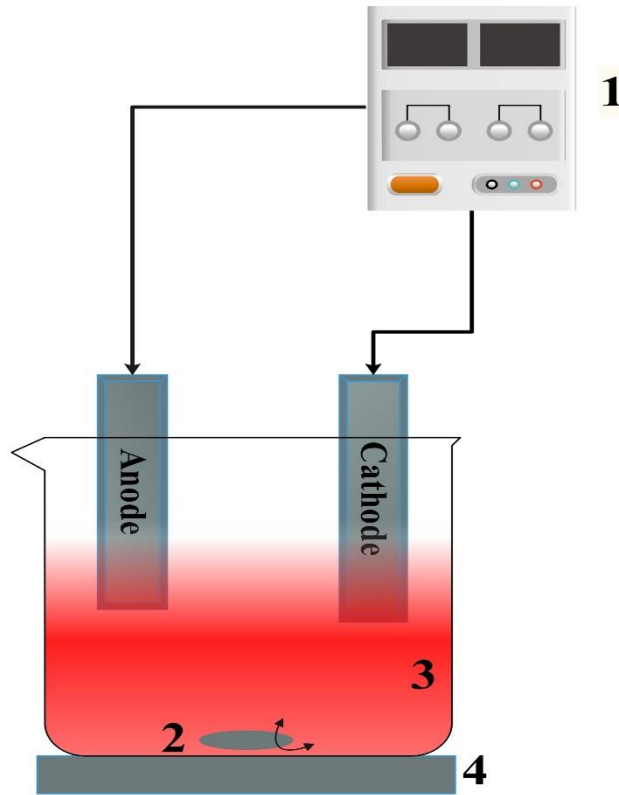


Fig. 1 Schematic Diagram of EC cell: (1) DC supply, (2) Magnetic Bar, (3) Dye polluted wastewater sample, (4) Magnetic stirrer.

2.4 Analytical Procedure

The initial absorbance of wastewater was measured by scanning the dye solution through UV-vis Spectrophotometer (Optima SP-3000). Decolorization (%) was calculated using following equation:

$$\text{Decolorization}(\%) = \frac{\lambda_o - \lambda}{\lambda_o} \times 100 \quad (5)$$

Where λ_o is the initial absorbance of azo dye before treatment process while λ is final absorbance of treated sample.

Chemical Oxygen Demand (COD) was measured by closed reflux colorimetric method after digestion of samples in COD thermal reactor. COD removal % was calculated as follows:

$$\text{COD}(\%) = \left(1 - \frac{\text{COD}_f}{\text{COD}_o} \right) \times 100 \quad (6)$$

Where COD_f is the final COD value of treated sample while COD_o is the initial COD of wastewater sample. The iron content of the treated samples were measured through flame

atomic absorption spectroscopy (Shimadzu AA-6800). The instrumental parameters were tuned according to manufacturer's recommendations. The flame was composed of acetylene (gas pressure 15kg/cm²) and air (gas pressure 1 kg/cm²). For determining iron content in treated samples, stock standard iron solutions of 2mg/L, 5mg/L and 10mg/L were prepared for comparative study and iron concentrations of optimized samples were measured. Deuterium (D2) lamp was used as radiation source. Distilled water was used after performing each iron content analysis in Flame Atomic absorption Spectrophotometry for washing purposes. Subsequently, current efficiency(ϕ_{Fe}) of Fe dissolution, described as a ratio of weight amount of Fe present in the solution or flocs at time t, m_{Fe} , over that produced by anodic dissolution based on Faraday's Law as three electrons are generated per single Fe ion formed, can be calculated as: [19]

$$\Phi_{Fe} = \frac{m_{Fe}}{M_{Fe} \times \frac{60It}{3F}} \quad (7)$$

Where M_{Fe} is the molar mass of Iron, I is amount of constant current supplied in the process, t is the total duration of electrocoagulation and F is the Faraday constant.

2.5 Experimental Design and Response Surface Methodology

The operating variables which were considered in electrocoagulation process are pH, initial concentration of dye, inter-electrode distance, concentration of electrolyte, electrode surface area and voltage. However, the independent variables for electrocoagulation of azo dye are pH, inter-electrode distance and initial concentration of dye as they have a direct effect on the responses and these variables were considered for process optimization and attain maximum achievable results of desired responses involving operating parameters. Moreover, the selection of these parameters was based on the ability to impart major impacts on electrocoagulation process. The experiments were designed using Design Expert (Stat-Ease, Inc, Version 10.0.1) software. Response Surface Methodology was used to explore the control variables along with their individual and combined effects on multiple responses. Response Surface Methodology consists of various statistical and mathematical methods which relates model fitness based on predicted data and experimental values relative with experimental design. In order to achieve desired objective, linear or quadratic polynomial functions are implemented to illustrate desired system and explore experimental conditions involving operating parameters until process optimization is configured [20]. Central Composite Design from Response Surface Methodology (RSM) was used as a suitable model of optimization in order to observe the behavior of responses by investigating selected variables at three different

levels. Central Composite Design (CCD) is a competitive statistical design that was chosen for the process optimization in which 20 set of experiments were designed. The experiments were based upon face centered central composite design involving three numeric factors with six replicas of central points simultaneous with fourteen factorial and axial points. The experiments were run in order to find the optimal measurements of responses that were chosen as COD reduction and decolorization. The response can be expressed in an equation of second-order model as follows:

$$Y = \beta_o + \sum_{i=1}^k \beta_i X_i + \sum_{i=1}^k \beta_{ii} X_i^2 + \sum_{i=1}^k \sum_{j=1}^k \beta_{ij} X_i X_j + \varepsilon \quad (8)$$

In equation (7) Y is the measurement of the response. β_o is the constant co-efficient while β_i , β_{ii} and β_{ij} are the co-efficients of linear, quadratic and second order terms respectively. X_i and X_j can be termed as variables. Values of co-efficients are very significant in order to estimate the importance of operating variables in each response. Negative co-efficient of independent variables implies that increase in operating variable shows a decreasing trend of particular response values. **Table 1** shows the levels and ranges of independent variables along with the coded values.

Table 1: Ranges and Levels of Independent Variables

Variables	Parameters	Levels		
		-1	0	-1
A	Dye Con. (mg/L)	500	750	1000
B	Inter-Electrode Distance (cm)	2	3	4
C	pH	3	6	9

CHAPTER 3: RESULTS AND DISCUSSION

3. Results and Discussion

3.1 Model Development and Statistical Analysis

In order to investigate the effect of independent variables (initial concentration of dye pollutant (mg/L), Inter Electrode Spacing (cm) and pH) on responses including COD reduction (%) and decolorization (%), 20 set of experiments were carried out as designed by Response Surface Methodology (RSM). Under RSM, Central Composite Design (CCD) method was employed with 8 factorials, 6 axials, and 6 center points values were recommended by the software. CCD method is a significant statistical tool that is commonly used in order to form second order response surface statistical model in process optimization studies [21]. CCD is considered as an efficient substitute of full factorial design as it manages to provide accurate statistical data by initiating less number of experiments [22]. The complete design matrix involving all values of responses (COD (%) and Decolorization (%)) integrated from the RSM model are presented in Table 2. Based on the experimental results, second order polynomial model was developed to predict the performance of the process. The functions of both responses that have been selected for this electrocoagulation process are given in equations (9) and (10).

$$\text{COD Reduction (\%)} = Y_1 = 51.91 - 8.30A + 0.25B - 12.86C + 0.26AB + 2.07AC + 2.56BC - 12.98A^2 - 5.69B^2 + 27.05C^2 \quad (9)$$

$$\text{Color removal (\%)} = Y_2 = 98.12 - 0.44A + 0.13B - 0.67C - 0.29AB - 0.16AC - 0.04BC + 1.09A^2 - 2.56B^2 + 0.93C^2 \quad (10)$$

Where A is the initial concentration of dye, B is the inter-electrode spacing and C is the initial pH of solution. The main purpose of developing this empirical model was to adequately illustrate the interaction of independent variables on the responses [23]. Based on the results as provided in Table.2, The observed efficiencies of COD reduction and decolorization were varied between 13.6% - 86.3% and 96% - 100% respectively.

Table 2 Factors and Responses from RSM

Run	Initial Conc. Of Dye	Electrode Spacing	pH	Experimental Values	
				Color Removal	COD Reduction
	mg/L	cm		%	%
1	1000 (+1)	2(-1)	9(+1)	97	36.23
2	750(0)	4(+1)	6(0)	96	39.41
3	750(0)	3(0)	6(0)	97.87	55.60
4	750(0)	3(0)	6(0)	98.12	51.42
5	750(0)	3(0)	3(-1)	100	85.42
6	750(0)	3(0)	6(0)	98.3	51.51
7	750(0)	3(0)	9(+1)	98	67.53
8	750(0)	3(0)	6(0)	98.13	59.74
9	500(-1)	3(0)	6(0)	100	44.32
10	1000(+1)	4(+1)	3(-1)	98	63.10
11	750(0)	3(0)	6(0)	98.26	51.22
12	1000(+1)	4(+1)	9(+1)	96	45.24
13	500(-1)	2(-1)	3(-1)	98.2	86.36
14	750(0)	3(0)	6(0)	98.21	51.90
15	500(-1)	2(-1)	9(+1)	97	50.00
16	500(-1)	4(+1)	3(-1)	98.5	84.09
17	500(-1)	4(+1)	9(+1)	98	56.82
18	750(0)	2(-1)	6(0)	95.02	48.05
19	1000(+1)	3(0)	6(0)	98.32	28.57
20	1000(+1)	2(-1)	3(-1)	98	65.48

Quadratic regression model is selected as highly significant model since they have very low levels of probability ($p < 0.01$). The significance and validation of coefficient associated with each operating parameter can be calculated from the p-values that are listed in Table.3. From Table.3 it is evident that model Y_1 terms A, C, A^2 and C^2 have significant effects on COD reduction efficiency while model Y_2 terms A, C, A^2 and C^2 have a significant effect on the color removal efficiency of the process. It can be also concluded from the table that Y_1 term B^2 and Y_2 term AB considered as marginally significant on COD reduction and Color removal efficiencies respectively as their p-values less than 0.1 but less than 0.05 ($0.05 < p < 0.1$).

Table 3 Regression estimate of selected model for COD reduction and Color removal

Relationship	Factors	Co-efficient	prob>F	Remarks
COD Reduction (Y ₁)				
Linear	Model	51.91		
	A	-8.29	0.002	Significant
	B	0.25	0.8637	
	C	-12.86	<0.0001	Significant
Quadratic	A ²	-12.98	0.0008	Significant
	B ²	-5.69	0.0652	Marginally Significant
	C ²	27.05	<0.0001	Significant
Interaction	AB	0.26	0.875	
	AC	2.07	0.229	
	BC	2.56	0.1432	
Color removal (Y ₂)				
Linear	Model	98.12		
	A	-0.44	0.0051	Significant
	B	0.13	0.321	
	C	-0.67	0.0003	Significant
Quadratic	A ²	1.09	0.0009	Significant
	B ²	2.56	<0.0001	Significant
	C ²	0.93	0.0026	Significant
Interaction	AB	-0.29	0.0623	Marginally Significant
	AC	-0.16	0.2632	
	BC	-0.04	0.79	

Mathematical model equations that are developed after adjusting the function to experimental values may not give accurate results[24]. In order to check the validation of empirical models developed through RSM, a statistical technique Analysis of Variance (ANOVA) was employed. The validation of a model can be done through five parameters, namely the Prob > F of the model, the lack of fit test, adequate precision, Adjusted Regression Co-efficient (Adj. R²) and the regression coefficient (R²). The values of Prob > F indicates if the empirical model is significant enough, lack of fit signifies the fitness of the model. Adequate Precision measures the signal to noise ratio. Regression co-efficient determines the effect of selected parameters on the whole model and Adjusted R² is advance form of Regression Co-efficient that has been adjusted for the number of predictors in the model.

If the value of "Prob > F" is less than 0.0500, it indicates that model terms are significant. Non-significance Lack of fit model is usually good since we want the model to be fit. Adequate Precision of greater than 4 is desirable whereas if the values of R² and Adj. R² are close, it defines the accuracy of the model. As from Table 4, models of COD and decolorization have

fulfilled the criteria and can be used to predict the performance of the process. Moreover, the adequacy of models for both responses can be assessed by creating a diagnostic plot between predicted values and actual values that were obtained through experimentation. The plots indicate that the data points lie very close to the diagonal line which shows the minimum residual for the prediction of each selected response. Fig 2 (a) –(b) shows the plot of actual vs predicted values of COD reduction and Color removal efficiencies respectively. Therefore, after the evaluation of Anova analysis and adequacy of models. the results showed an efficient agreement between experimental and theoretical data

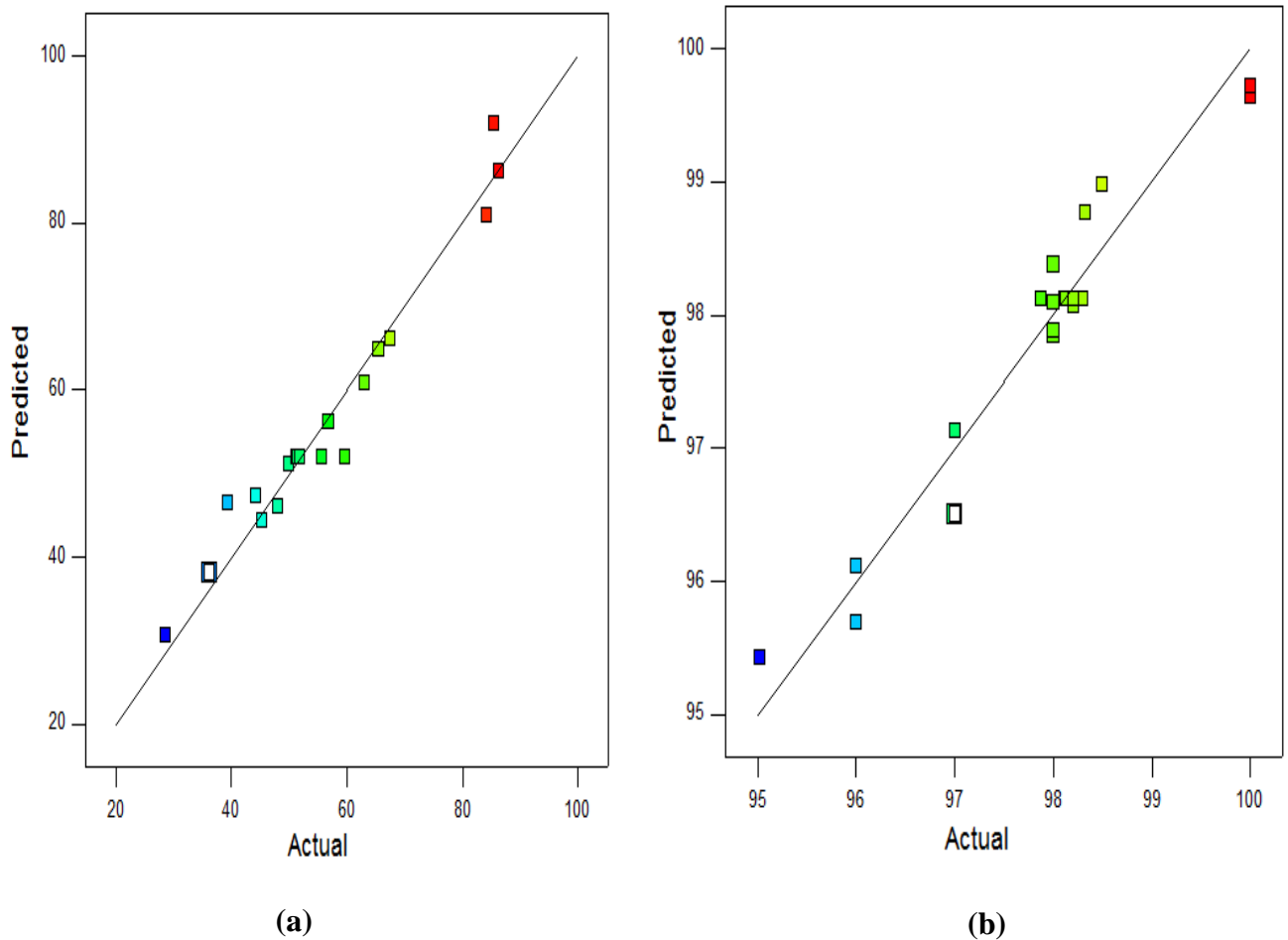


Fig. 2 Actual vs predicted values plot for testing Adequacy of developed regression models describing (a) COD reduction (b) Color Removal Efficiency of EC Process

Table 4. ANOVA analysis for %COD and %Decolorization for EC process

Response	Source	SS ^a	Df ^b	MS ^c	F-value ^d	Prob>F	
COD Reduction	Model	4507.11	9	500.79	24.10	< 0.0001	
	Linear	2311.91	11	210.17	17.69	0.0027	
	Quadratic	148.41	5	29.68	2.50	0.1689	
	Interaction	2224.82	8	278.10	23.41	0.0015	
	Residual	207.82	10	20.78			
	Lack of fit	148.41	5	29.68	2.50	0.1689	
	Pure error	59.41	5	11.88			
	Total	4714.93	19				
	Adequate Precision = 18.982						
	R ² =95.62%; adjust R ² = 91.61%						
Color Removal	Model	25.55	9	2.84	18.89	< 0.0001	
	Linear	20.36	11	1.85	78.51	< 0.0001	
	Quadratic	1.39	5	0.28	11.75	0.0086	
	Interaction	19.48	8	2.43	103.27	< 0.0001	
	Residual	1.50	10	0.15			
	Lack of fit	1.39	5	0.28	11.75	0.0086	
	Pure error	0.12	5	0.024			
	Total	27.05	19				
	Adequate precision = 15.642						
	R ² =94.44%; adjust R ² = 89.44%						

^a SS= sum of squares

^b Df= Degree of freedom

^c MS= Means square

^d F-value= Value of variance

3.2 Pareto Analysis

Graphical Pareto Chart and analysis is another significant technique to validate model selection and demonstrate the contribution of operating variables to understand the obtained output value of selected responses [25]. In this study, this graphical tool is selected in order to obtain the percentage contribution of each control factor on COD reduction and Color removal efficiency which were considered as desired responses. The equation of pareto analysis can be expressed as follows:[26]

$$P_i = \frac{b_i^2}{\sum b_i^2} \times 100 \text{ (if } i \neq 0) \quad (11)$$

Here b_i shows the estimation of significance of operating parameters as indicated by second-degree polynomial equation. According to Fig. 3, interaction effect of pH (C^2) has most significant influence of 62.12% on COD reduction efficiency. Similarly, interaction effect of Inter-electrode distance (B^2) has most substantial contribution on Color removal efficiency with 69.89%. Linear effect of initial concentration of dye (A) in COD reduction efficiency can be expressed as 5.85% while its quadratic effect can be calculated as 12.67% in Color removal efficiency. Out of all variables, Interactive effect of all correlative variables (AB, BC and AC) have weak percentage contribution in both COD reduction and color removal efficiency as Interactive contribution within COD reduction efficiency was obtained as 0.01%,0.35% and 0.56% from AB, BC and AC respectively. In color removal efficiency, interactive effect of AB is marginally significant than rest of correlative effects (AC and BC) with percentage contribution of 1% while AB and AC effect in color removal efficiency are 0.27% and 0.02% respectively. On the basis of pareto chart, it is configured that pH induce most significant contribution on COD removal and Decolorization[27, 28]. Additionally, Inter-electrode spacing also plays an important role on the COD removal along with pH of the solution[29].

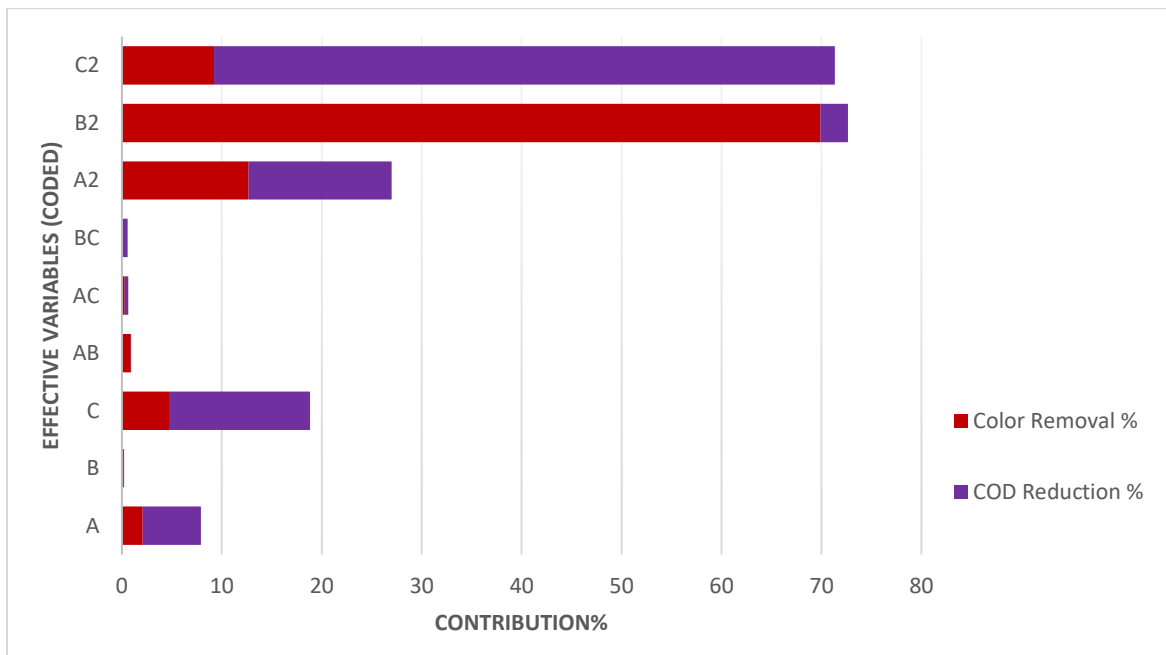
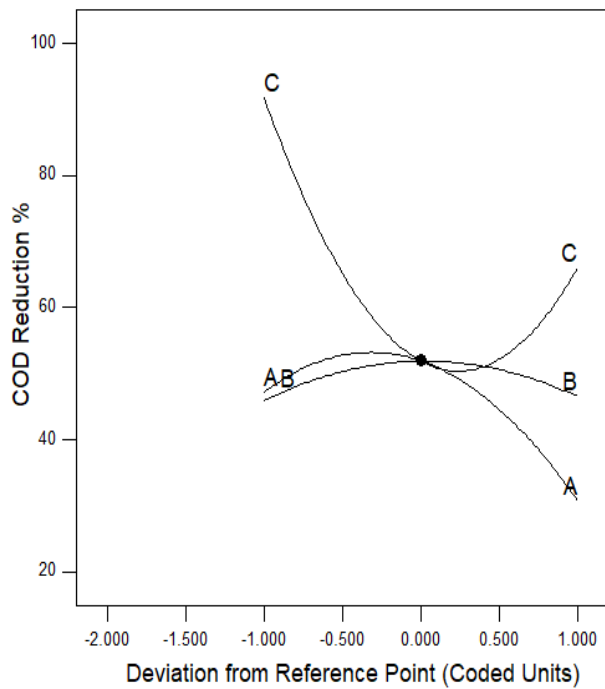


Fig. 3 Graphical Pareto Plot of independent variables on selected responses

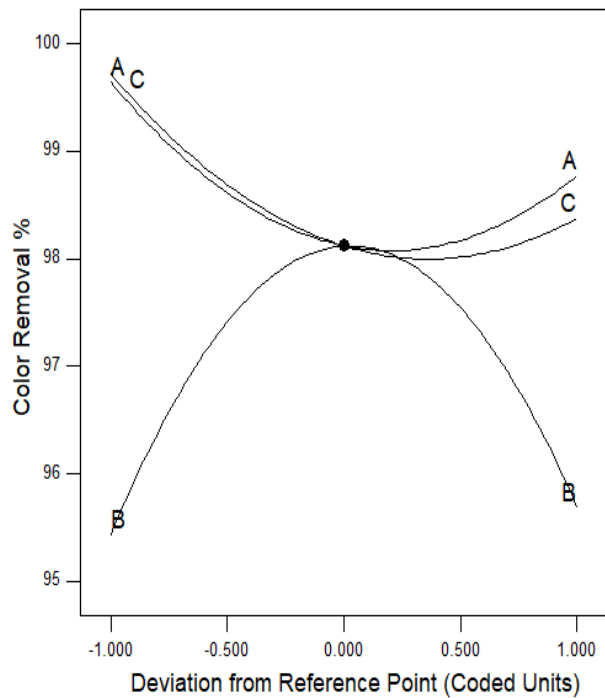
3.3 Perturbation Plots

Perturbation Plots is another efficient graphical method which is implied in order to compare the effect of control factors at the specific point in design space. In perturbation plots, responses are plotted by changing values of one factor within selective range while other factors are held

constant. The significance of operating factor with respect to selected response is determined by observing the steepness of the curvature of respective factor. In this study, the plots are selected within center of space (Initial concentration of dye (A) = 750 mg/L; Inter-Electrode Spacing (B)= 3 cm; pH (C) = 6). Hence, two Perturbation plots were obtained since the only two responses that were considered are COD reduction and Color removal efficiency. It can be seen from Fig.4 that both Color removal efficiency and COD reduction are sensitive to all the factors that are involved in this study. However, initial concentration of dye is the only factor that has been less sensitive in both response as compared to remaining factors. In COD reduction efficiency, pH (C) factor imparts most important effect on response since steeper lines with curvature shows the sensitivity to the change in factor. However, inter-electrode spacing (B) implies deepest effect on the sensitivity of other response called Color removal efficiency. Thus, it can be concluded from the perturbation plots that pH (C) and inter-electrode distance (B) has most significant effect on COD reduction and Color removal efficiency respectively while initial concentration of dye (A) is less sensitive in both responses. Previous studies also proves the validation of perturbations plots regarding the contribution of pH and inter-electrode distance as more significant operating parameters on COD reduction and color removal efficiency in electro-coagulation process[30, 31].



(a)



(b)

Fig. 4 Perturbation Plots at center point of design space for (a) COD reduction efficiency (b) Color removal efficiency. *Where A, B and C represents Initial concentration of dye (mg/L), Inter-electrode spacing (cm) and pH

3.4 Effect of Operating Parameters

The effects of three operating parameters namely initial pH of solution, Inter-electrode spacing and initial concentration of dye were studied using RSM. RSM is a statistical design method used to study the effect of selected parameters over the selected responses such as % decolorization and % COD removal. The effects of operating parameters on required responses are investigated by three-dimensional response surface plots. 3D response surface plots give a clear analysis about interactive effects of variables as compared to conventional two-dimensional plots. The trend of individual operating variable on %Decolorization and %COD are explained separately. The main findings of these contour plots are presented in **Table 5.**

Table 5. Effect of operating parameters on %COD and %Decolorization

Operating parameters			Responses	
Initial concentrations of dye (mg/L)	pH	Inter-electrode distance (cm)	COD (%)	Decolorization (%)
Effect of pH				
500	3-9	3	89.15-59.1 (decrease)	101.79-100.06 (decrease)
500-1000	3	3	89.15-68.59 (decrease)	101.79-100.52 (increase)
1000	3-9	3	68.59-46.65 (decrease)	100.52-98.86 (decrease)
Effect of Inter-electrode distance				
500	9	2-4	50-56.82 (increase)	97-98 (increase)
500-1000	9	2	50-36.23 (decrease)	97-97 (No effect)
1000	9	2-4	36.23-45.24 (increase)	97-96 (decrease)
Effect of Interelectrode distance (If I.E distance of 3cm is included since its optimum value is 3cm)				
500	9	2-3	50-59.35 (increase)	97.12-99.71 (increase)

500	9	3-4	59.35-56.82 (decrease)	99.71-97.91 (decrease)
1000	9	2-3	36.23-47.04 (increase)	96.49-98.85 (increase)
1000	9	3-4	47.04-45.24 (decrease)	98.85-96.49 (decrease)

3.4.1 Effect of initial pH

Based on the findings of experimental results along with statistical methods such as ANOVA and perturbation plots, initial pH seems to show significant contribution to electrocoagulation process. Fig. 5 (b-c) and Fig. 6 (b-c) shows the effect of initial pH on %COD and %Decolorization respectively. As observed, higher %COD and %Decolorization were achieved if pH of the solution was acidic and decreased when initial pH was gradually changed from acidic to basic. As reported in Table 5, change of pH value from 3 to 9 at fixed inter-electrode distance (3cm) and initial concentration of dye (500mg/L), %COD decreases from 89.15% to 59.1%. %Decolorization shows the similar decreasing trend from 101.79% to 100% if pH increases from acidic to basic medium. Similarly, at higher concentration of dye (1000mg/L), availability of electron is reduced and %COD decreases from 68.59% to 46.65% if pH is increased from 3 to 9. The inter-electrode distance has been kept fixed at 3cm. %Decolorization also shows decreasing trend from 100.52% to 98.86% in similar conditions. These results are also supported by the study of Khorram et al. [32] in which maximum %COD and %Decolorization was achieved at acidic pH of the solution. Parsa et al.[33] also removed 91% of dye content and 87% of %COD when EC is employed for treatment of Acid Brown 14 from wastewater. The higher values of selected responses at lower pH value can be described due to formation of monomeric species which serves as efficient coagulants for treatment of dye enriched wastewater [34]. In acidic solutions, these monomeric iron anions are present in large amount. When electric potential is applied on iron electrode, redox reaction occurs in which iron is oxidized at anode and converted to Fe^{+3} ions while hydrogen gas is liberated along with hydroxyl ions at cathode. Redox reactions can be explained in the following equations: [35]

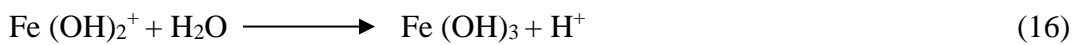
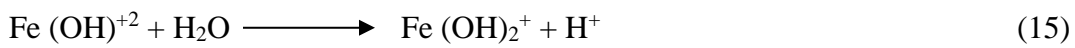
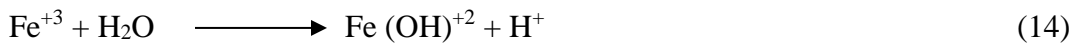
Anodic reaction:



Cathodic reaction:



After generation of Fe^{+3} ions, it produces various monomeric coagulants along with hydroxides as their concentration is largely dependent on the pH of the solution. The forthcoming reactions for the generations of monomeric species and hydroxides can be described as follows:



The high COD reduction efficiency can be related to the presence of monomeric species like Fe (OH)^{+2} , Fe(OH)_2^{+} , Fe (OH)_4^{-} and Fe(OH)_3 . Fe(OH)_3 has an efficient coagulant capacity in the treatment of Congo red dye as it possesses large surface area to absorb dye molecules regarded as pollutants [36]. When pH of solution is shifted to basic condition, these monomeric species are converted to complex polymeric molecules such as $\text{Fe}_2(\text{OH})_2^{4+}$ and $\text{Fe}_6(\text{OH})_{15}^{3+}$ due to presence of large number of hydroxyl groups. Fe(OH)_3 is generally dissolve at higher pH values due amporism phenomenon and therefore it possess poor solubility when solution is basic. This phenomenon is also observed by Daneshever et al. [37] in which it is stated that complex species like Fe(OH)_4^{-} holds poor tendency to form coagulants due to its dissolving nature. Besides investigating the significant influence of initial pH on the selected responses, Table.5 also shows that dye concentration has inverse effect on %COD and %Decolorization. It is observed that if dye concentration is kept at 500mg/L at constant inter-electrode spacing (3cm) under acidic conditions, 89.15% of %COD was achieved. However, when amount of initial concentration of dye pollutant is increased to 1000mg/L, %COD diminishes significantly up to 68.59% under similar conditions (Inter-electrode spacing=3cm; initial pH=3). The reason behind this decreasing trend is due to the fact that since current density in each experimental run is constant as equal number of amperes has been provided using DC supply, Faraday's law states that equal amount of Fe^{+3} can be passed into the dye polluted solution if current density is constant [38]. Consequently, the amount of coagulants formed in each experimental run are same in number. Therefore, it can be observed that the coagulants

of Fe^{+3} ions which are formed at higher concentration have poor tendency to capture dye particles. %Decolorization also shows similar decreasing trend as of %COD if amount of dye concentration is enhanced [39].

3.4.2 Effect of Inter-electrode spacing

Besides initial pH of the wastewater sample, statistical analysis also identifies that inter-electrode spacing plays a significant effect on desired responses. The ranges of Inter-electrode spacing used in this study are 2-4 cm. The effect of inter-electrode spacing on %COD and %Decolorization are shown through 3D contour plots of Fig. 5 (a-b) and Fig.6 (a-b) respectively. Through observation, it is concluded that rate of %dye removal initially increases if distance between two electrodes is increased between 2 and 3cm. This statement is also supported by Table.5 in which if initial concentration of dye and pH are fixed at 500mg/L and 9 respectively and inter-electrode spacing is altered between 2-3cm, %COD increases considerably from 50-59.35%. Similarly, %Decolorization also increases from 97.12-99.71% within same conditions. This result is also supported by Huda et al. [40] in which EC study was implemented on landfill leachate and high values of %COD and %Decolorization were achieved if distance between electrode were kept around 3cm. To support this finding, Yoriya et al. interpreted that ionic transport in EC process takes place due to electric field generated between two electrodes. The decrease in inter-electrode distance increases electrode pore size as a result of which the capability of oxide formation and chemical dissolution process improves at the same time. Hence, the large dissolution of iron electrodes is observed[41]. However, if inter-electrode spacing is further increased beyond 3cm, %COD and %Color decreases. Table.5 indicates that %COD and % Decolorization decreased from 59.35-56.82% and 99.71-97.91% respectively if inter-electrode spacing is enhanced from 3-4cm with fixed pH (9) and initial concentration of dye (500mg/L). Similar trends were observed if fixed concentration of dye is changed to 1000mg/L. This decreasing trend is due the fact that at far distance of inter-electrode spacing, the pore size is decreased. The decrease in pore size might have been caused due to increased voltage drop which raises the power consumption along the path of current provided in the electrolytic solution that is used in the EC system[42]. Electric potential between the electrodes decreases if the spacing between the electrodes is increased. This phenomenon is also observed during performing experimental runs, whereby increase of inter-electrode spacing enhances the voltage of EC process. Therefore, by managing optimum distance between electrodes, the energy consumption and operating cost

could be managed economically. The inter-electrode spacing also influences the current density distribution as current density decreases with decrease in inter-electrode spacing due to low internal resistance[43]. However, if the inter-electrode distance is established below 2cm, rate of %COD and %Decolorization declines because transfer of solid and fluid material is hindered. Due to this obstruction, the resultant solid particles and bubbles generated between two electrodes causes higher electrical resistance[44]. It is also observed that along with effect of inter-electrode spacing, %COD and %Decolorization can also be affected by initial concentration of dye concurrently. Table.5. suggests that if initial concentration of dye is varied at 500mg/L-1000mg/L while other operating parameters are kept constant (Inter-electrode spacing=4cm ; pH=9), %COD decreases from 56.82% to 45.24%. This significant decrease in %COD by increasing dye concentration is due to high voltage drop which is caused by internal resistance of solution. The ohmic resistance of solution is increased if cathode is moved further away from anode. The ohmic resistance of electrolyte R can be expressed as following eq. 17:[45]

$$R = \frac{d}{A} \frac{1}{k} \quad (17)$$

Where “d” denotes the distance between two electrodes, “A” is surface area of electrodes while “k” is the conductivity of solution. According to Ohm’s law, Conductivity of a solution is decreased if voltage is boosted. Hence, solution with higher concentration of dye has weaker conductivity as compared to lower concentration of dye. According to eq. (17), lower conductivity of a solution generates higher voltage drop which decreases %COD due to boosted resistance of solution [46].

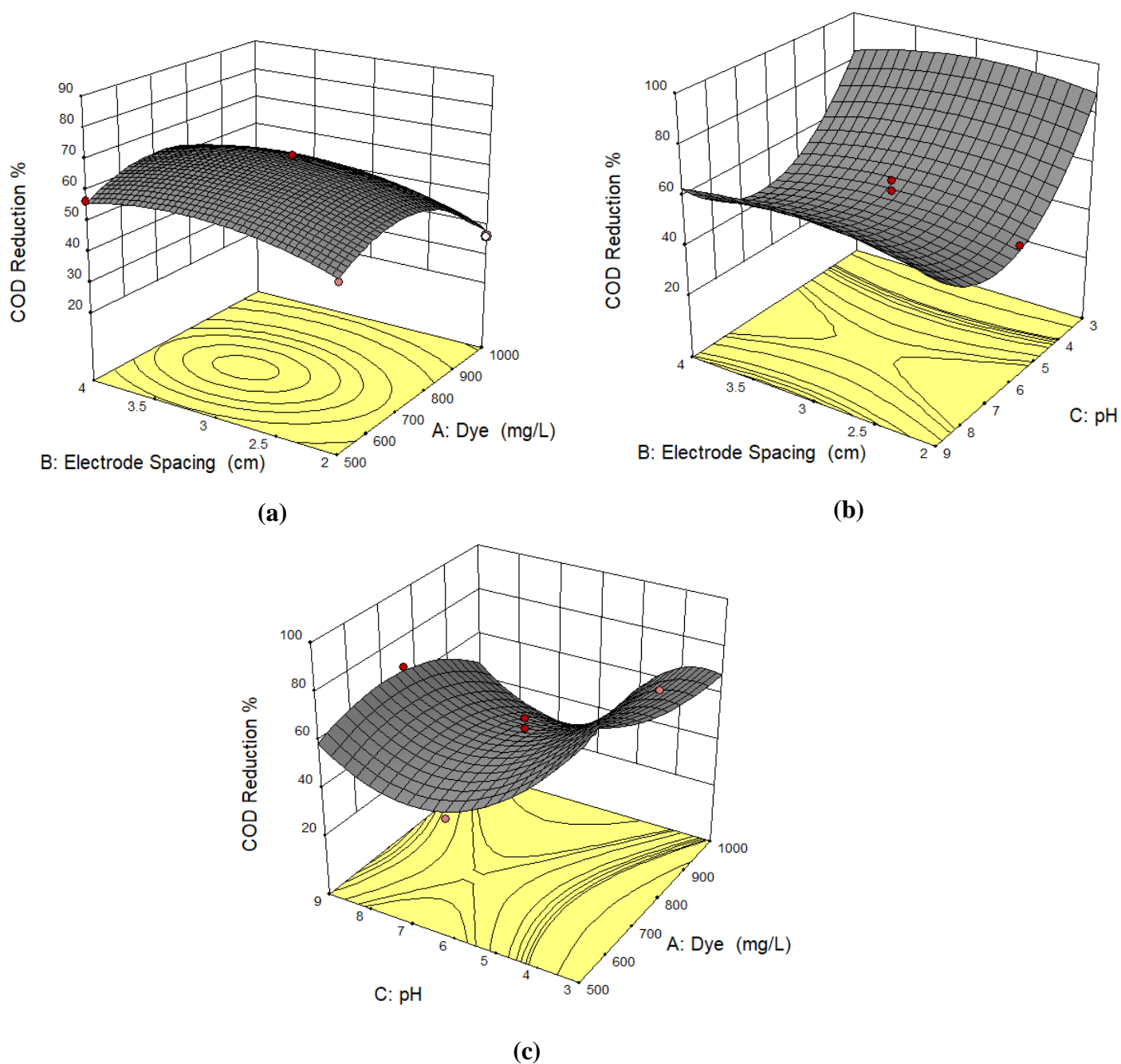


Fig. 5 Three-dimensional response surface plots of %COD reduction between (a) electrode spacing and initial concentration of dye (b) electrode spacing and pH (c) pH and initial concentration of dye

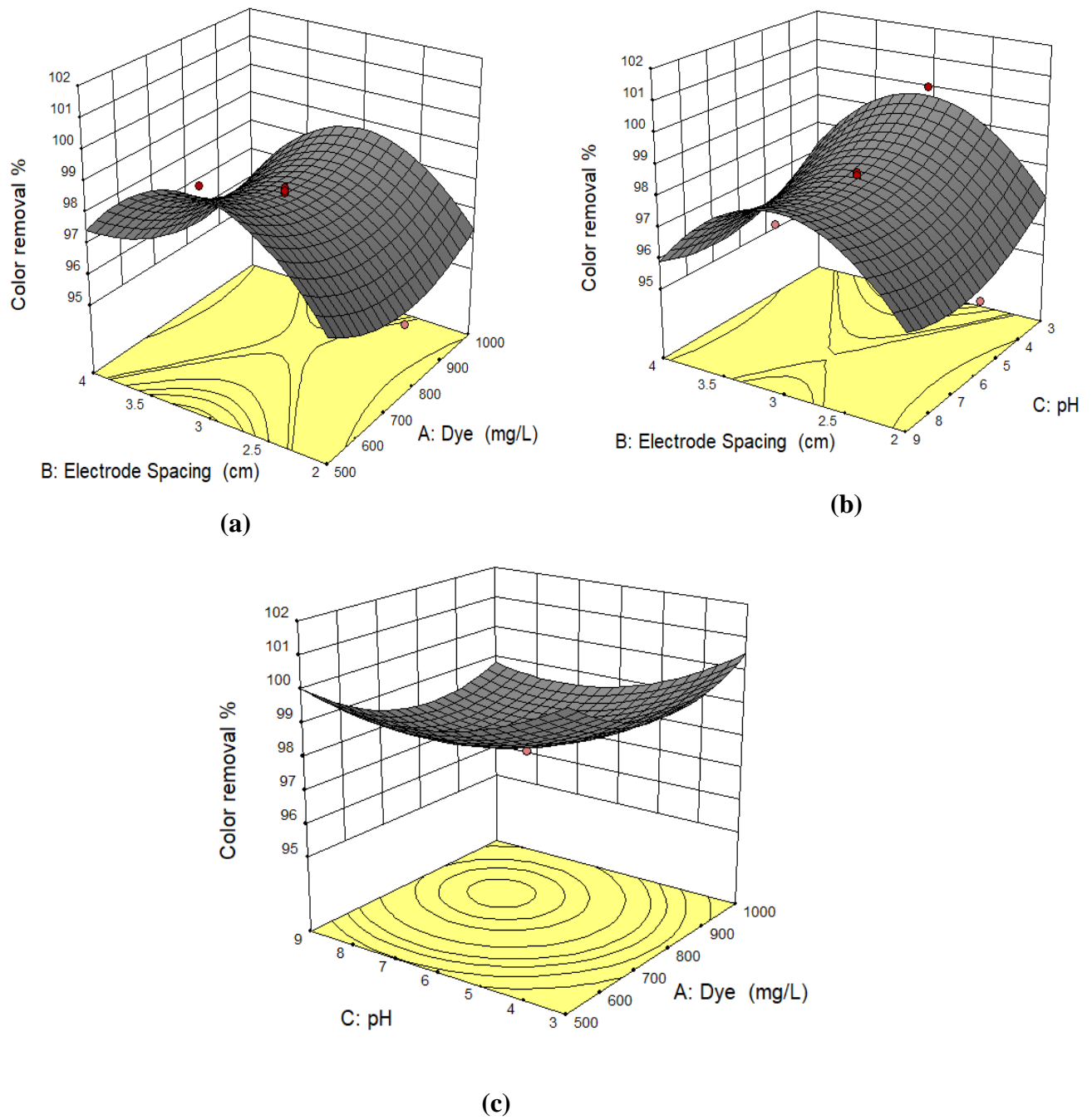


Fig. 6 Three-dimensional response surface plots of %Decolorization between (a) electrode spacing and initial concentration of dye (b) electrode spacing and pH (c) pH and initial concentration of dye

3.5 Optimization including desirability and kinetic analysis

Optimization of operating parameters is an essential part in process development as basic purpose of present work was to find optimum conditions that yields maximum %COD and %Decolorization. In order to pursue numerical optimization, desirability function approach was utilized. Since the optimum values of three operating values were different, desirability function is an efficient method in order to attain maximum output values of selected responses like %COD and %Decolorization. For %COD, highest and lowest achievable value was considered as 28.57% (minimum experimental value) and 91.82% (maximum theoretical value) respectively. Same procedure was implied for %Decolorization as 95.02% was selected since it is minimum experimental value while 100% was selected as it was the maximum value that has been achieved successfully by experimentation. In Design Expert Software, the values of operating parameters (Inter-electrode distance, pH) were kept in range while initial dye concentration were targeted as 1000 mg/L in order to find out optimum conditions at highest concentration of Congo red dye. The %COD and %Decolorization were set at maximum. The experiment which possess highest amount of desirability was selected to validate the optimum conditions. Table.6 shows the optimum conditions with the predicted and actual values performance of the electrocoagulation. At operating conditions of 3, 2.8 cm and 1000 mg/L of initial pH, inter-electrode spacing and initial dye concentration respectively, the experimental results yielding %COD and %Decolorization are close in agreement to predicted results which confirms the validity of model. The economic values are an important factor in optimization for electrocoagulation process. Electrical energy consumption and current are very important economical parameters in EC process. Electrical consumption can be calculated as follows: [47]

$$e = V \times I \times t \quad (18)$$

Where E is the electrical energy (Wh) consumed in EC process. V is the cell voltage provided through DC supply, I is the amount of current in the process and t is the electrolysis time. It has been observed that if EC process is set up when electrode spacing is greater than 3cm it accumulates considerable amount of voltage. Since current and time of electrocoagulation process is constant, if voltage in the process, the energy consumption of EC process also increases considerably. In order to calculate electrical energy consumed for removal of 1g of dye pollutant, following relationship is employed:

$$E = \frac{e}{C_0 - C} \quad (19)$$

Where E (Wh/g) is the total electrical energy consumed for removal of 1g of dye pollutant while Co and C are the COD concentration of initial sample and treated sample respectively.

By employing Electrocoagulation process, maximum %COD of 89% was achieved and %Decolorization was 97% under optimum conditions. The good agreement between predicted and actual values also validates the assigned model. Fig.7 shows the behavior of %COD and %Decolorization with the respect to electrolysis time by using optimum values of controlled parameters. It can be easily observed from the trend that %COD and %Decolorization of dye enriched wastewater increases by decreasing electrolysis time under optimum conditions. With increase in electrolysis time, soluble monomeric species like Fe (OH)₃, which is considered to be efficient coagulant, is converted into polymeric coagulants which have poor capability to coagulate with the dye pollutant. Moreover, pH within the electrocoagulation process increases with the passage of time as compared to initial pH due to constant inclusion of hydroxyl group in dye solution and this gradual increase of pH plays significant role in poor tendency for the removal of dye pollutant.

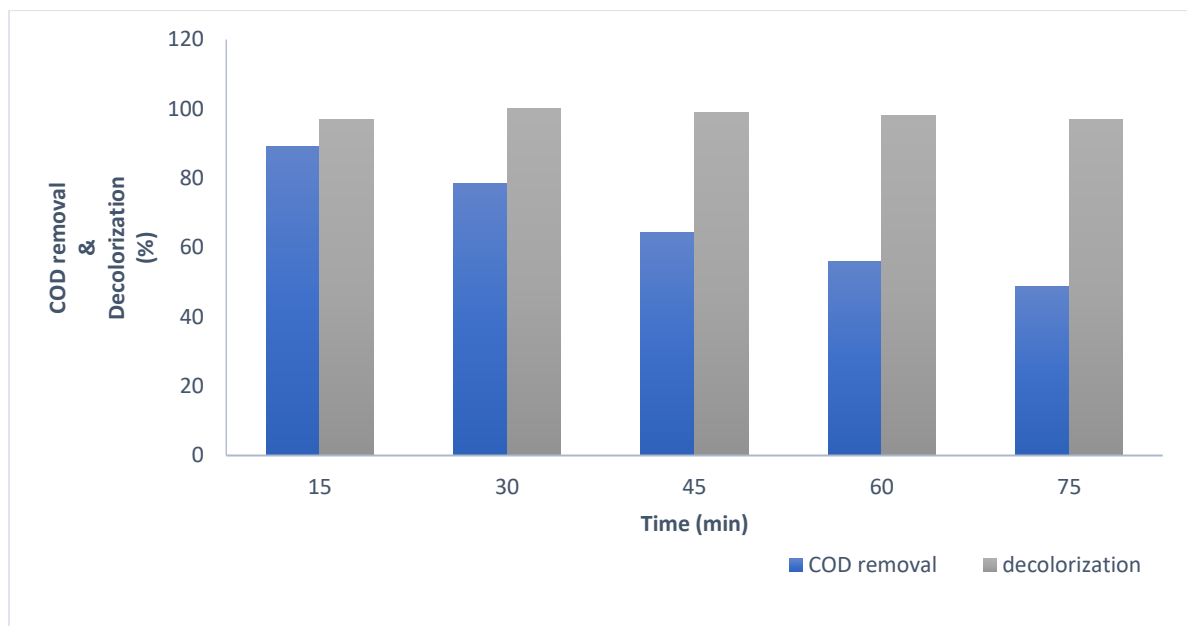


Fig. 7 EC Performance with respect to electrolysis time (pH=3; I.E Spacing= 3cm; Initial concentration of dye=1000 mg/L)

Table. 6 Values of numerical optimization

Initial pH	Inter-electrode Spacing (cm)	Initial Concentration of dye (mg/L)	%COD		%Decolorization	
			Pred.	Exp.	Pred.	Exp.
3	3	1000	87	89	100	97

The kinetic study for the removal of dye pollutant from wastewater can be expressed with the following zero-order, first-order equation and second order reactions (eq. (20-22)): [48]

Zero-Order Reaction:

$$\left(\frac{dc}{dt}\right) = -k_o \quad (20)$$

First-Order Reaction:

$$\left(\frac{dc}{dt}\right) = -k_1C \quad (21)$$

Second-Order Reaction:

$$\left(\frac{dc}{dt}\right) = -k_2C^2 \quad (22)$$

Where C represents the COD value of the solution whereas k_0, k_1, k_2 represents the kinetic rate constants of zero-order, first-order and second-order reactions respectively while t represents the reaction time.

After integrating the preceding equation, following equations are obtained:

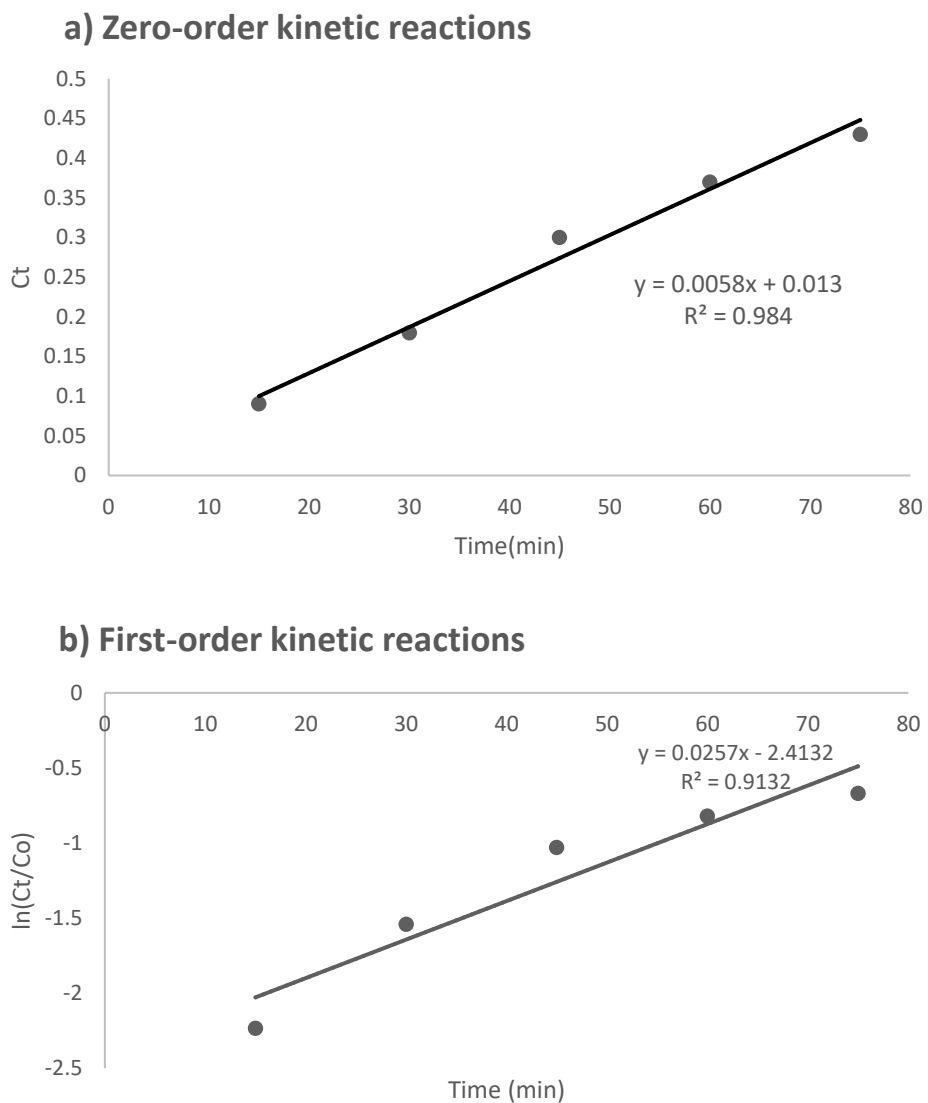
$$C_t = -k_0t + C_o \quad (23)$$

$$\ln C_t = -k_1t + \ln C_o \quad (24)$$

$$\frac{1}{C_t} = k_2t + \frac{1}{C_o} \quad (25)$$

Where C_0 and C_t shows the initial COD of dye enriched wastewater solution and concentration of treated solution at any time respectively.

The regression-based analysis including zero-,first- and second-order kinetic analysis was conducted for the removal of COD from wastewater solution. The results are presented in Fig.8. It is observed that zero-order kinetic model (Fig. 10(a)) has regression co-efficient $R^2=0.984$, which gives much higher value as compared to regression co-efficients of first-order kinetics ($R^2=0.981$) and second-order kinetics ($R^2=0.7891$). After obtaining the regression co-efficients through graphical representation, it can be concluded that zero-order kinetic model fits the reaction more efficiently than other applied kinetic models. The rate order of zero order kinetics $k_0= 0.0058 \text{ s}^{-1}$ was calculated from the resultant slope. This result is also supported by the kinetic study of Cortes et al. in which it is concluded that zero order kinetic model perfectly fits the kinetic degradation of acid blue 9 by using TiO_2/UV advanced oxidation process.[49]



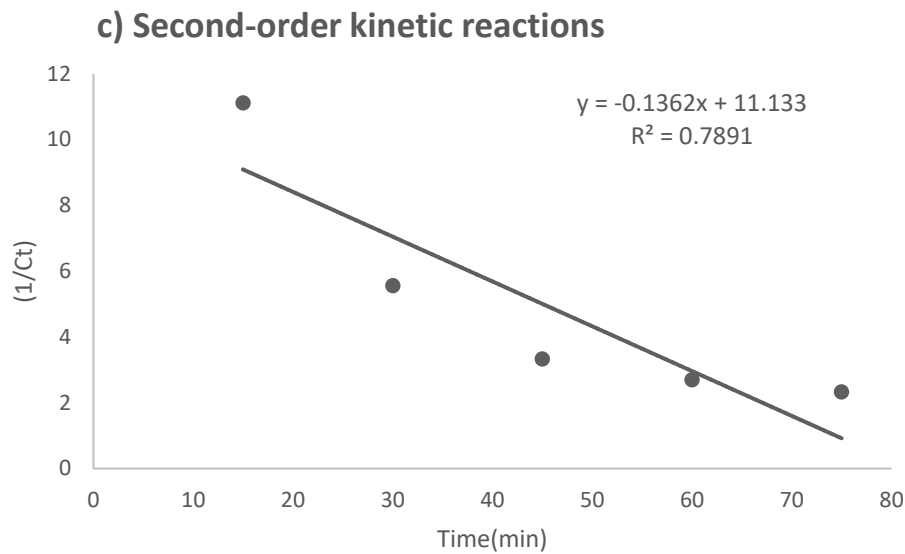


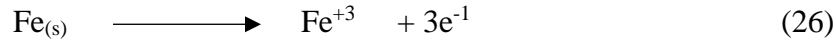
Fig. 8 Graphical Plots of a) Zero-order b) First-order and c) Second-order Kinetic Models for COD reduction under optimum parameters (Initial Concentration of dye=1000mg/L ; Initial pH=3 ; Inter-electrode distance=2.8 cm)

3.6 Concentration of residual iron post EC Process

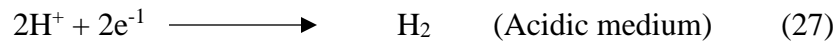
Iron electrode releases ferric ions at anode region during EC process and these ions reacts with hydroxyl ions in water in order to form coagulants including $\text{Fe}(\text{OH})_3$ [50] along with polymeric complex species such as $\text{Fe}(\text{OH})_4^-$ and $\text{Fe}_6(\text{OH})_{15}^{+3}$ [51]. However, Fe ions fails to form coagulants or complex hydroxyl compounds and remains in the treated solution as secondary pollutant[52]. In order to measure iron content within treated solution, samples were analyzed under Flame Atomic Adsorption Spectroscopy (Shimadzu- AA6800). Standard iron solutions of 2 mg/L, 5 mg/L and 8 mg/L were formed in order to find out the absorbance of iron content. Afterwards, iron concentrations of 5 samples were measured after employing EC process. The values of two operating parameters (initial pH and Inter-Electrode spacing) were varied in each experimental run from 3-9 and 2-4cm respectively. However, value of initial concentration of Congo red dye was kept constant in all experiments. Table.7 shows iron concentration in each experiment that were performed for iron content analysis. It can be observed from Table.7 that maximum iron concentration of 7.56 mg/L was measured in acidic solution and spacing between electrodes were 2cm. The reason behind maximum content of iron in acidic condition is due to the fact that in acidic condition the hydroxyl ions are less as

compared to basic conditions. The high iron concentration of Iron can be explained under following equation[40]:

At Anode:



At Cathode:



It can be clearly observed from eq. (27) and eq. (28) that hydroxyl ions are present in higher quantity within alkaline medium. Whenever pH of the solution is increased, Iron ions precipitates out in the form of coagulants such as $\text{Fe}(\text{OH})_3$ and other polymeric species of iron coagulants[53]. However, large amount of residual iron are unable to form complex polymeric coagulants in acidic conditions due to insufficient hydroxyl ions[54]. Apart from initial pH, inter-electrode spacing plays an important role on release of iron content. It is also observed from Table.7. that the amount of iron content is maximum when inter-electrode distance too close. This is due to the fact that if electrode are brought too close to each other, the mass transfer between solid and fluid material is obstructed due to high electrical resistance[55]. Due to resistance in solid and fluid transfer, concentration of residual iron is increased.

The minimum concentration of iron were observed as 0.4 mg/L under 6 pH and Inter-electrode spacing were set at 3cm. The concentration of iron content in all experiments meets the US-EPA legislative standards for maximum allowable concentration of iron discharged wastewater(8mg/L). However, this treated solution is not entirely safe for drinking purposes since National Secondary Drinking Water Regulations (NSDWRs), founded by EPA, has set the secondary maximum contaminant level (SMCL) for iron at 0.3 mg/L. Although US-EPA states that excess of iron content above 0.3mg/L can only change aesthetic (color, odor and taste) effects of water and doesn't impart adverse consequences on human health. Fig.9 also shows graphical plots between iron concentration and values of operating parameters in each experimental run.

Table.7. Concentration of iron residual against varied operating parameters

Experiment	pH	I.E distance	Dye	Concentration of iron	Absorbance	EPA Standards for Iron discharge in drinking and industry effluents
		cm	mg/L	Ppm	A	ppm
1	3	4	1000	0.71	0.012	2-8* [56]
2	6	3	1000	0.40	0.0069	0.3 [57]
3	9	3	1000	7.10	0.1202	
4	3	2	1000	7.56	0.1297	
5	3	3	1000	1.02	0.0173	

*EPA Standards are with respect to countries. Therefore, range of standards for Iron discharge is calculated

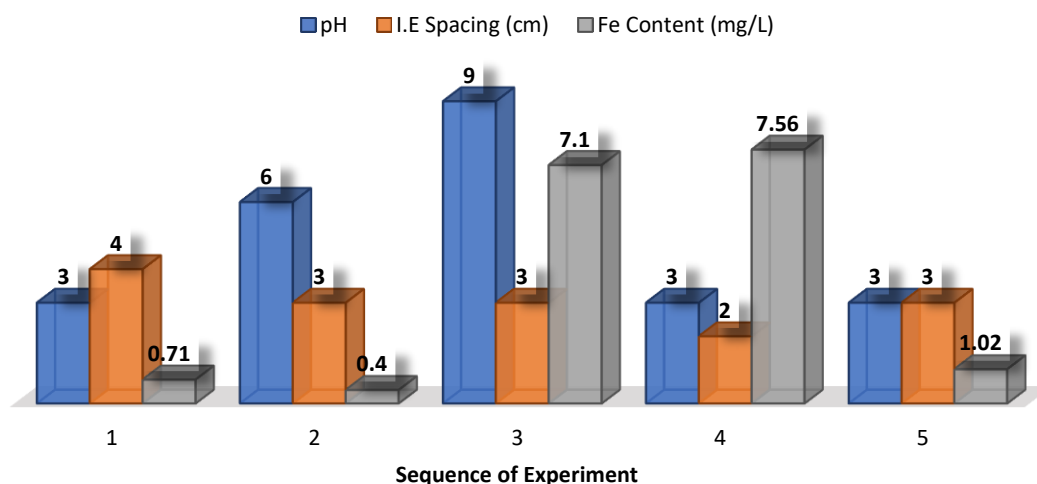


Fig. 9. Concentration of Residual with respect to different sequence of experiments

3.7 FTIR Analysis of Standard dye and Residual Sludge

The peaks in the spectrum of standard dye exhibit different groups present in congo red (a), as shown in figure. The characteristic peak at 3458 cm^{-1} may attribute to the stretching vibrations of $-\text{OH}$ group and/or N-H which correspond to NH_2 group of standard dye[58-60]. The peaks appeared within the band range of $1400\text{-}1650\text{ cm}^{-1}$ can be attributed to the aromatic carbon vibrations and/or azo group ($-\text{N}=\text{N}-$, $-\text{N-H}$)[58-62]. A peak due to C-N stretch vibration of the aromatic primary amine can be observed at 1349 cm^{-1} . It may also indicate $-\text{CH}_3$ out of plane

bending vibrations in the sample[59, 60, 62]. Additional peaks observed within band range of 1000-1200 cm^{-1} may indicate the presence of S=O and SO^{3-} asymmetric and symmetric stretching vibration due to sulfonic salt group. The group of peaks situated in the range 830-580 cm^{-1} could be attributed to the aromaticity or benzene rings which corresponds to naphthalene substituted rings[58-62].

A substantial variation in these peaks can be observed in the spectrum of sludge powder (b) indicate the degradation of dye pollutant in the presence of coagulant species that are generated due to iron electrode material[58, 61]. The intensity of all peaks appeared in standard dye decreased due to the formation of dye-metal complex in the sludge. The stretching vibrations of azo group turn to the asymmetric and symmetric bending vibrations of N-H correspond to primary amine[60]. A broadness of peak at 1114 cm^{-1} confirms the existence of SO_3H , which may be attributed to the interaction between SO_3^{3-} and H^+ . The oxidation of iron forms FeOOH and $\text{Fe}(\text{OH})_2$ in an aqueous solution which leads to the formation of H^+ and SO_3H [62].

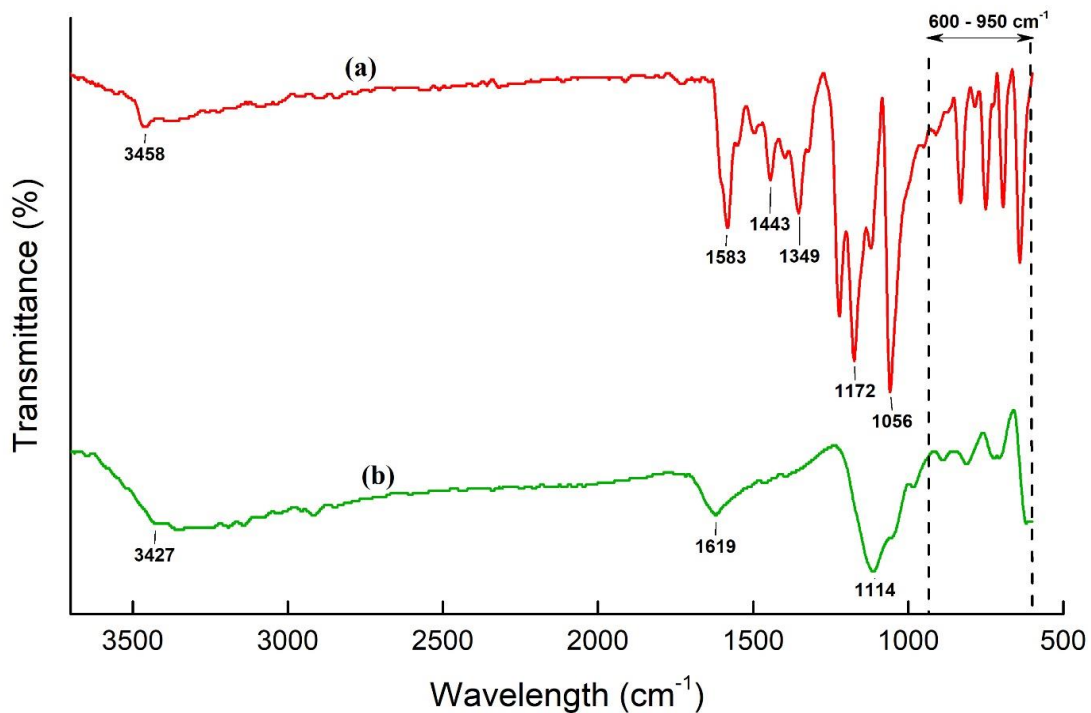


Fig. 10. FTIR Spectra of Standard Congo Red dye (a) and Residual Sludge (b) obtained after EC process (pH=3; Inter-electrode spacing= 3cm ; Initial concentration of dye= 1000 mg/L)

4. Conclusion

The performance of electrocoagulation process for the treatment of dye laden wastewater was studied. The effects of initial concentration of dye, initial pH and inter-electrode distance were investigated on COD reduction and color removal efficiencies. After extensive experimentation and statistical analysis, inter-electrode distance and initial pH were considered as most significant parameters for COD reduction and color removal efficiency. Under optimum conditions (initial pH=3; inter-electrode spacing=3cm; initial concentration of dye=1000mg/L) 89% of COD reduction efficiency and 97% of color removal efficiency were achieved successfully. The models of second-order polynomials selected for the process were able to predict COD reduction and color removal with a good agreement between experimental and predicted values. The EC process is viable for the possibility of zero water discharge and reuse of dye in various departments within textile sector.

5. References

1. Brillas, E. and C.A. Martínez-Huitle, *Decontamination of wastewaters containing synthetic organic dyes by electrochemical methods. An updated review*. Applied Catalysis B: Environmental, 2015. **166**: p. 603-643.
2. Khandegar, V. and A.K. Saroha, *Electrocoagulation for the treatment of textile industry effluent—a review*. Journal of environmental management, 2013. **128**: p. 949-963.
3. Koch, M., et al., *Ozonation of hydrolyzed azo dye reactive yellow 84 (CI)*. Chemosphere, 2002. **46**(1): p. 109-113.
4. Mohan, N., N. Balasubramanian, and C.A. Basha, *Electrochemical oxidation of textile wastewater and its reuse*. Journal of hazardous materials, 2007. **147**(1-2): p. 644-651.
5. Freitas, T., et al., *Optimization of coagulation-flocculation process for treatment of industrial textile wastewater using okra (A. esculentus) mucilage as natural coagulant*. Industrial Crops and Products, 2015. **76**: p. 538-544.
6. Yavuz, Y. and Ü. Ögütveren, *Treatment of industrial estate wastewater by the application of electrocoagulation process using iron electrodes*. Journal of environmental management, 2018. **207**: p. 151-158.
7. Li, X., et al., *Landfill leachate treatment using electrocoagulation*. Procedia Environmental Sciences, 2011. **10**: p. 1159-1164.
8. Akyol, A., *Treatment of paint manufacturing wastewater by electrocoagulation*. Desalination, 2012. **285**: p. 91-99.
9. Varank, G., et al., *Electrocoagulation of tannery wastewater using monopolar electrodes: process optimization by response surface methodology*. International Journal of Environmental Research, 2014. **8**(1): p. 165-180.
10. Katal, R. and H. Pahlavanzadeh, *Influence of different combinations of aluminum and iron electrode on electrocoagulation efficiency: Application to the treatment of paper mill wastewater*. Desalination, 2011. **265**(1-3): p. 199-205.

11. Kobya, M., et al., *Treatment of potable water containing low concentration of arsenic with electrocoagulation: Different connection modes and Fe–Al electrodes*. Separation and Purification Technology, 2011. **77**(3): p. 283-293.
12. Golder, A., A. Samanta, and S. Ray, *Removal of trivalent chromium by electrocoagulation*. Separation and purification technology, 2007. **53**(1): p. 33-41.
13. İrdemez, Ş., N. Demircioğlu, and Y.Ş. Yildiz, *The effects of pH on phosphate removal from wastewater by electrocoagulation with iron plate electrodes*. Journal of hazardous materials, 2006. **137**(2): p. 1231-1235.
14. Franco, D., et al., *Removal of phosphate from surface and wastewater via electrocoagulation*. Ecological Engineering, 2017. **108**: p. 589-596.
15. Verma, A.K., *Treatment of textile wastewaters by electrocoagulation employing Fe-Al composite electrode*. Journal of Water Process Engineering, 2017. **20**: p. 168-172.
16. Can, O., et al., *Treatment of the textile wastewater by combined electrocoagulation*. Chemosphere, 2006. **62**(2): p. 181-187.
17. GilPavas, E., I. Dobrosz-Gómez, and M.Á. Gómez-García, *Optimization of sequential chemical coagulation-electro-oxidation process for the treatment of an industrial textile wastewater*. Journal of water process engineering, 2018. **22**: p. 73-79.
18. Alinsafi, A., et al., *Electro-coagulation of reactive textile dyes and textile wastewater*. Chemical engineering and processing: Process intensification, 2005. **44**(4): p. 461-470.
19. Elabbas, S., et al., *Treatment of highly concentrated tannery wastewater using electrocoagulation: influence of the quality of aluminium used for the electrode*. Journal of hazardous materials, 2016. **319**: p. 69-77.
20. Bezerra, M.A., et al., *Response surface methodology (RSM) as a tool for optimization in analytical chemistry*. Talanta, 2008. **76**(5): p. 965-977.
21. Aksoy, D.O. and E. Sagol, *Application of central composite design method to coal flotation: Modelling, optimization and verification*. Fuel, 2016. **183**: p. 609-616.
22. Aslan, N., *Application of response surface methodology and central composite rotatable design for modeling the influence of some operating variables of a Multi-Gravity Separator for coal cleaning*. Fuel, 2007. **86**(5-6): p. 769-776.
23. Iftikhar, M., et al., *Biomass densification: Effect of cow dung on the physicochemical properties of wheat straw and rice husk based biomass pellets*. Biomass and Bioenergy, 2019. **122**: p. 1-16.
24. Körbahti, B.K., *Response surface optimization of electrochemical treatment of textile dye wastewater*. Journal of hazardous materials, 2007. **145**(1-2): p. 277-286.
25. Cheng, L.-C., et al., *Application of response surface methodology for electrochemical destruction of cyanide*. International Journal of Physical Sciences, 2012. **7**(44): p. 5870-5877.
26. Ahmadzadeh, S., et al., *Removal of ciprofloxacin from hospital wastewater using electrocoagulation technique by aluminum electrode: optimization and modelling through response surface methodology*. Process Safety and Environmental Protection, 2017. **109**: p. 538-547.
27. Bashir, M.J., et al., *Post treatment of palm oil mill effluent using electro-coagulation-peroxidation (ECP) technique*. Journal of Cleaner Production, 2019. **208**: p. 716-727.
28. GilPavas, E., I. Dobrosz-Gómez, and M.-Á. Gómez-García, *Optimization and toxicity assessment of a combined electrocoagulation, H₂O₂/Fe²⁺/UV and activated carbon adsorption for textile wastewater treatment*. Science of the Total Environment, 2019. **651**: p. 551-560.
29. Bouhezila, F., et al., *Treatment of the OUED SMAR town landfill leachate by an electrochemical reactor*. Desalination, 2011. **280**(1-3): p. 347-353.
30. Naje, A.S., et al., *Electrocoagulation using a rotated anode: A novel reactor design for textile wastewater treatment*. Journal of environmental management, 2016. **176**: p. 34-44.

31. Ilhan, F., et al., *Treatment of leachate by electrocoagulation using aluminum and iron electrodes*. Journal of hazardous materials, 2008. **154**(1-3): p. 381-389.
32. Khorram, A.G. and N. Fallah, *Treatment of textile dyeing factory wastewater by electrocoagulation with low sludge settling time: Optimization of operating parameters by RSM*. Journal of environmental chemical engineering, 2018. **6**(1): p. 635-642.
33. Parsa, J.B., et al., *Removal of Acid Brown 14 in aqueous media by electrocoagulation: Optimization parameters and minimizing of energy consumption*. Desalination, 2011. **278**(1-3): p. 295-302.
34. Pajootan, E., M. Arami, and N.M. Mahmoodi, *Binary system dye removal by electrocoagulation from synthetic and real colored wastewaters*. Journal of the Taiwan Institute of Chemical Engineers, 2012. **43**(2): p. 282-290.
35. Mondal, B., et al., *Parametric and multiple response optimization for the electrochemical treatment of textile printing dye-bath effluent*. Separation and Purification Technology, 2013. **109**: p. 135-143.
36. Mollah, M.Y.A., et al., *Electrocoagulation (EC)—science and applications*. Journal of hazardous materials, 2001. **84**(1): p. 29-41.
37. Daneshvar, N., A. Oladegaragoze, and N. Djafarzadeh, *Decolorization of basic dye solutions by electrocoagulation: an investigation of the effect of operational parameters*. Journal of hazardous materials, 2006. **129**(1-3): p. 116-122.
38. Daneshvar, N., et al., *Decolorization of CI Acid Yellow 23 solution by electrocoagulation process: Investigation of operational parameters and evaluation of specific electrical energy consumption (SEEC)*. Journal of hazardous materials, 2007. **148**(3): p. 566-572.
39. Khemila, B., et al., *Removal of a textile dye using photovoltaic electrocoagulation*. Sustainable Chemistry and Pharmacy, 2018. **7**: p. 27-35.
40. Huda, N., et al., *Electrocoagulation treatment of raw landfill leachate using iron-based electrodes: effects of process parameters and optimization*. Journal of environmental management, 2017. **204**: p. 75-81.
41. Yoriya, S., *Effect of inter-electrode spacing on electrolyte properties and morphologies of anodic TiO₂ nanotube array films*. Int. J. Electrochem. Sci, 2012. **7**(9454): p. e9464.
42. Hashim, K.S., et al., *Electrocoagulation as a green technology for phosphate removal from river water*. Separation and Purification Technology, 2019. **210**: p. 135-144.
43. Faria, P., M. Hallett, and P.C. Miranda, *A finite element analysis of the effect of electrode area and inter-electrode distance on the spatial distribution of the current density in tDCS*. Journal of neural engineering, 2011. **8**(6): p. 066017.
44. Sridhar, R., et al., *Treatment of pulp and paper industry bleaching effluent by electrocoagulant process*. Journal of hazardous materials, 2011. **186**(2-3): p. 1495-1502.
45. Hakizimana, J.N., et al., *Electrocoagulation process in water treatment: A review of electrocoagulation modeling approaches*. Desalination, 2017. **404**: p. 1-21.
46. Malakootian, M., H. Mansoorian, and M. Moosazadeh, *Performance evaluation of electrocoagulation process using iron-rod electrodes for removing hardness from drinking water*. Desalination, 2010. **255**(1-3): p. 67-71.
47. Daneshvar, N., A. Khataee, and N. Djafarzadeh, *The use of artificial neural networks (ANN) for modeling of decolorization of textile dye solution containing CI Basic Yellow 28 by electrocoagulation process*. Journal of hazardous materials, 2006. **137**(3): p. 1788-1795.
48. Buthiyappan, A., A.A.A. Raman, and W.M.A.W. Daud, *Development of an advanced chemical oxidation wastewater treatment system for the batik industry in Malaysia*. RSC Advances, 2016. **6**(30): p. 25222-25241.
49. Cortés, J.A., et al. *Kinetic degradation of acid blue 9 through the TiO₂/UV advanced oxidation process*. in *The Nanotechnology Conference and Trade Show (NSTI Nanotech)*, Santa Clara. 2007.

50. Nandi, B.K. and S. Patel, *Effects of operational parameters on the removal of brilliant green dye from aqueous solutions by electrocoagulation*. Arabian Journal of Chemistry, 2017. **10**: p. S2961-S2968.
51. Gengec, E., et al., *Optimization of baker's yeast wastewater using response surface methodology by electrocoagulation*. Desalination, 2012. **286**: p. 200-209.
52. Aytac, E. and U.T. Un, *Removal of Reactive Scarlet Dye and COD Using Cylindrical Iron Rod Anodes In A Semi-Continuous Reactor*. International Journal of Scientific Research in Science & Technology, 2018. **4**(8).
53. Mohajeri, S., et al., *Landfill Leachate Treatment through electro-Fenton oxidation*. Pollution, 2019. **5**(1): p. 199-209.
54. Bayramoglu, M., M. Eyvaz, and M. Kobya, *Treatment of the textile wastewater by electrocoagulation: economical evaluation*. Chemical Engineering Journal, 2007. **128**(2-3): p. 155-161.
55. Phalakornkule, C., S. Polgumhang, and W. Tongdaung, *Performance of an electrocoagulation process in treating direct dye: batch and continuous upflow processes*. World Academy Sci. Technol, 2009. **57**: p. 277-282.
56. Agency, U.S.E.P. *US-EPA Standards for wastewater discharge effluents 2002* [cited 2017 December]; Concentration of iron in wastewater discharge]. Available from: <https://www.epa.gov/eg/industrial-wastewater-treatment-technology-database-iwtt>.
57. Agency, U.S.E.P. *Secondary Drinking Water Standards: Guidance for Nuisance Chemicals*. 2002 19 January 2017 [cited 2010 March]; Available from: <https://www.epa.gov/dwstandardsregulations/secondary-drinking-water-standards-guidance-nuisance-chemicals>.
58. Aoudj, S., et al., *Electrocoagulation process applied to wastewater containing dyes from textile industry*. Chemical Engineering and Processing: Process Intensification, 2010. **49**(11): p. 1176-1182.
59. Lafi, R., I. Montasser, and A. Hafiane, *Adsorption of congo red dye from aqueous solutions by prepared activated carbon with oxygen-containing functional groups and its regeneration*. Adsorption Science & Technology, 2019. **37**(1-2): p. 160-181.
60. Luntraru, V., et al. *Synthesis and characterization of Congo red adsorbed onto titanium dioxide-iron composite*. in *CAS 2011 Proceedings (2011 International Semiconductor Conference)*. 2011. IEEE.
61. Raghu, S., et al., *Evaluation of electrochemical oxidation techniques for degradation of dye effluents—A comparative approach*. Journal of Hazardous Materials, 2009. **171**(1-3): p. 748-754.
62. Kim, S.-H. and P.-P. Choi, *Enhanced Congo red dye removal from aqueous solutions using iron nanoparticles: adsorption, kinetics, and equilibrium studies*. Dalton Transactions, 2017. **46**(44): p. 15470-15479.